Jestr

Journal of Engineering Science and Technology Review 17 (3) (2024) 27 - 38

Research Article

JOURNAL OF
Engineering Science and Technology Review

www.jestr.org

Good Matching Broad-band Frequency Acoustic Duct Lined with Parabolic Increasing Microperforated Area

F. B. Shenoda and M. Y.El Aidy*

Department of Acoustics, National Institute of Standards, Tersa Str, Al-Haram, El-Giza, P.O.B:136 code 12211, Egypt.

Received 24 December 2023; Accepted 3 June 2024

Abstract

Despite the increasing interest in acoustic silencer design for various noise control applications, the good matching performance duct design has not been getting much interest. The present work gives the theoretical study and the experimental verification of the matching performance to plane sound waves in a one-dimensional duct lined with a parabolic increasing microperforated area. The wave propagation inside the duct is modelled using the boundary element method (BEM), and its solution is derived using the modified Hankel function. The matching performance, namely the wave impedance, and the sound reflection coefficient at the duct inlet were computed when this duct is inserted between two similar hard ducts. Ducts lined with different duct parameters of length, cross-section diameter, graduality of the wall conductance of different micro-perforation characteristic parameters were considered. The wave impedance and the sound reflection coefficient of a single slit treatment, at the duct inlet were theoretically studied and discussed. Also, ducts of multiple treatments by equal and similar slit areas of micro-perforation were studied. The theoretical study of the proposed duct design shows that the matching performance can be improved by tuning both duct parameters and MPP liner physical characteristics, especially for liners in which the reactive part of its impedance is less or equal to its resistive part, and a reflection coefficient of less than 0.15 which is the reflection-free condition, is obtained in a wideband frequency from low frequency, from 200 Hz to the first high mode frequency in the duct. In comparing the theoretical and experimental measurement data, a reasonable agreement has been found for both the sound impedance and the sound reflection at the duct inlet.

Keywords: Silencer, Microperforated panels, Reflection coefficient, Acoustic impedance, Acoustic Matching, Sound Absorption.

1. Introduction

In industrial noise control, silencers, or mufflers are widely used to reduce the noise emitted from numerous sources such as internal combustion engines, fans, compressors, turbines, air conditioning systems, blowers, etc., [1]. Industrial mufflers are usually either reactive [2], dissipative [3], or hybrid [4] types. Reactive types are designed with multiple chambers and perforated tubes, in which, the attenuating sound is primarily by scattering and reflecting the sound waves towards the noise source [5], which suffers from impedance mismatching due to the discontinuity of the duct cross-section or abrupt change and causes high back pressure, which results in extra power consumption of the gas flow passes through it. The absorptive or dissipative type implies sound-absorbing materials, the noise reduction mechanism of this type is based on the absorption of sound wave energy through the absorbed materials, and converting it to heat, it is used normally for attenuating high-frequency sound. The resonant type possesses a narrow band of sound absorption and a relatively large volume. In general, the use of any type is usually restricted to special systems and purposes.

The noise reduction mechanism in absorptive silencers is based on the absorption of sound wave energy that propagates along the tube and converting it into heat through sound absorption materials. Hybrid silencers are constituted of absorbing and reactive parts to improve the performance of silencers [6].

The mismatching impedance of sound propagation is almost due to passing through ducts of cross-section with area discontinuity. Many situations are occurring in practice where sound propagates in such non-uniform ducts [7-8]. Optimization of this discontinuity has been achieved using the graduality effect [9-10]. Good matching acoustic impedances is an important goal in acoustics for particular applications, including the design of anechoic termination, mufflers, and aero-engine nacelle [11], different approaches for duct design were considered in literature [12-13]. Shenoda [14] designed a reflection-free air duct termination that gives a good matching impedance for acoustic plane sound waves traveling along a pipe of uniform cross-section. The basic concept of such termination is to provide a gradually changing flow resistance along the pipe wall. He realized it by a suitable gradually variable perforation of the pipe wall in combination with a sound-absorbing material. In a series of research, Shenoda et al. [15-16] and Shenoda [17-18] applied this concept and developed several sound attenuators, whose noise control is independent of the kind and performance of the noise source and has no influence on its performance.

Modelling sound wave propagation in pipe systems is important in the prediction of sound reflection. Wave propagation in ducts is modelled by most authors using the Finite Element method (FEM) [19-20], [21], Boundary Element Method (BEM) [22-23] or Transfer Element Method (TEM) [24-25].

*E-mail address: melaidy@yahoo.com
ISSN: 1791-2377
doi:10.25103/jestr.173.04

For cases where clean absorbent is desirable when mufflers must support high air flux or when a sound absorber is needed for severe environments, it is not possible to use traditional fibrous materials. In this kind of application, microperforated panels (MPPs) can be used as liners instead of fibrous materials, which provides high sound resistance and absorption. Such a panel is made of perforated metal sheets of perforation diameter in sub-millimeter, these plates provide enough acoustics resistance and enhance sound absorption. The MPP, which is made of a metallic plate is considered to be non-combustible and recyclable and is suitable for applications in a high-temperature environment [26].

The mismatching in ducts is due to the discontinuity of sound wave impedance throughout the duct, which is due to abrupt changes in the cross-section or the lining of the duct. A good design model proposed by Shenoda, has a constant cross-section area along the treated duct and is lined with variable lining increasing area.

The object of the present work is to give the theoretical study and the experimental verification to the matching performance of a duct that has a constant cross-section area along the treated duct and lined with parabolic increasing microperforated-area to a plane sound wave, (at frequencies below the cut-on for higher order modes) incident at duct inlet. It is also aimed to evaluate the duct parameters, and the MPP physical parameters of lining that affect the matching performance of the treated duct for the case of zero mean flow to give methods and tools that will enable the designer to achieve the optimum design goals. On the other hand, a good matching model realizes high sound attenuation, Shenoda and El-Aidy [27] studied and designed a one-dimensional duct of free constant cross-section area, whose wall is lined with a parabolic increasing microperforated area. This lined duct provides at certain conditions high sound attenuation at an effective low- to medium-frequency range.

2. Theoretical Treatment

The treated duct consists of a main tubular pipe of length *l* and has a constant free cross-section area *S*. The side wall of this main pipe is treated with a parabolic increasing homogeneously microperforated area. The maximum width of the micro-perforated area at the end of the treated duct is *Dm*. This area is produced from microperforated panels, MPP which have a thickness, *t*, hole diameter of perforation, *d* and a perforation ratio (porosity), σ. In some applications, the treated side is surrounded by a partitioned cavity of depth, *D*, Fig. 1a.

Maa [28-29] proposed an approximate equation for the normalized specific impedance of an *MPP*. It can be expressed as:

$$Z_{MPP} = R_m + j\,\omega m = R_m + jX_m \tag{1}$$

where,

$R_m = \frac{32\,\eta\,t}{\sigma\rho c d^2}\left[(1+\frac{\beta^2}{32})^{\frac{1}{2}} + \frac{\sqrt{2}}{32}\,\beta\,\frac{d}{t}\right]$, is the resistive part of Z_{MPP}, and

$X_m = \frac{\omega t}{\sigma c}\left[1 + (9+\frac{\beta^2}{2})^{-\frac{1}{2}} + 0.85\,\frac{d}{t}\right]$, is the reactive part of Z_{MPP}.

where,

c is the speed of sound, ω is the angular frequency;
ρ is the mass density of air;
η is dynamic viscosity of air = 1.789 x 10^{-5} kg/ms, and

$\beta = d\sqrt{\frac{\rho\omega}{4\eta}}$ which is called the perforate constant

From equation (1), it seems that Z_{MPP}, mainly relies on geometric parameters of the MPP (*t*, *d* and σ). In a previous work [29], the authors studied the effect of these parameters on both R_m and X_m.

The present work is engaged in the theoretical study of sound propagation in a finite one-dimensional duct lined at its side wall with a parabolic increasing microperforated area. In the theoretical treatment, some important assumptions were considered. It has been assumed that there is no flow through the system and sound pressures are small compared with absolute pressures, so linear equations are applicable. For such one-dimensional sound propagation in a lined duct, the wave equation for the velocity potential $\boldsymbol{u(x)}$ can be obtained by applying the fundamental field equations, namely the force and continuity equations. It can be expressed as

$$\frac{d^2u(x)}{dx^2} + \left[k_o^2 - j\left(\frac{k_o}{h_{eff}}\right)\rho c Y_m\right].u(x) \;= 0 \tag{2}$$

where:
*k*o is the wave number and equal *ω/c*,
ω is the angular frequency, *ω = 2πf*,
heff is the effective duct height =*S/D`*,
S is the duct cross-sectional area and *D'* is the lining width along the periphery.
$\rho c Y_m$ is the normalized local wall admittance of the treated side.

In our case, according to Fig. 1(b), the side of the duct is treated with a parabolic increase in axial direction microperforated area with its maximum width *Dm* at the output of the treated duct. Accordingly, we have.

$D` \implies D(x) = D_m.\sqrt{\frac{x}{l}}$, and

$$h_{eff} \implies h_{eff}(x) = \frac{S}{D(x)} = \frac{S}{D_m}\sqrt{\frac{l}{x}}, \tag{3}$$

Where,
Dx is the width of the parabolic increasing microperforated area of the treated side at point *x*,
Dm is the maximum width of the treated microperforated area at *x=l* and
l is the length of the treated duct.

Also, the normalized specific acoustic impedance of the wall at the treated side is changed parabolically in the axial direction according to the relation $\frac{Z(x)}{\rho c} = Z_{MPP}.\sqrt{l/x}$, and accordingly, the normalized admittance

$$\rho c Y_m(x) = \frac{1}{Z_{MPP}}.\sqrt{x/l} \tag{4}$$

Where,
$Z_{MPP} = R_m + j\,X_m$ is the normalized specific acoustic impedance of the microperforated panel,
MPP, from which the parabolic increasing microperforated area is produced.

Introducing equations (3) and (4) in equation (2) we have

$$\frac{d^2u(x)}{dx^2} + \left[k_o^2 - j\left({}^{k_o}/_{A_c}\right).x\right].u(x) = 0 \quad (5)$$

where,
$A_C = \frac{S.l.Z_{MPP}}{D_m}$ is the characteristic area of the treated duct

To solve this equation (5), we transfer it to a well-known differential equation form, that has a well-known solution. Accordingly, we use the following transformation, namely:

$z = -\ k_o\ A_c + jx,\ u(x) = u(z) = \sqrt{z}\ .\ Q(T)$, and

$$T = \frac{2}{3}\sqrt{\frac{k_o}{A_c}}\ .z^{3/2},$$

And have the differential equation

$$\frac{d^2Q(T)}{dT^2} + \frac{1}{T}.\frac{dQ(T)}{dT} + \left(1 - \frac{(1/3)^2}{T^2}\right).Q(T) = 0 \quad (6)$$

This is a BESSEL's differential equation of order one-third and has the closed-form solution:

$$Q(T) = C_1\ .H_{1/3}^{(1)}(T) + C_2\ .H_{1/3}^{(2)}(T)$$

Where *C1* and *C2* are arbitrary integration constants and $H_{1/3}^{(1)}(T)$ and $H_{1/3}^{(2)}(T)$ are Hankel-functions of the first and second kind [28] of complex argument *T* and order one-third. The two functions are triple-valued functions of *T*, with a branch point at the origin. However, the product of the two multiple-valued functions $T^{1/3}$ with $H_{1/3}^{(1\ or\ 2)}$ is the single-valued functions *h*1(z) or *h*2(z), which represents the modified Hankel functions of order one-third [31]. They are related to each other by the equations,

$$T^{\frac{1}{3}}\ H_{1/3}^{(1)}(T) = h_1\left(z.\sqrt[3]{\frac{k_o}{A_c}}\right)$$

$$T^{\frac{1}{3}}\ H_{1/3}^{(2)}(T) = h_2\left(z.\sqrt[3]{\frac{k_o}{A_c}}\right)$$

Accordingly, the complete solution of the differential equation (6) is given by,

$$Q(T) = C_1.T^{\frac{-1}{3}}\ .h_1(a.z) + C_2.T^{\frac{-1}{3}}\ .h_2(a.z)$$

$$u(x) = \sqrt{z}\ Q(T) = \sqrt{z}\ T^{-\frac{1}{3}}.[\ C_1\ h_1(a\ z) + C_2\ h_2(a\ z)]$$

This solution represents the incident as well as the reflected waves. For harmonic time dependence of the sound field, the sound pressure *pi*(*x*) and the sound particle velocity *vi* (*x*) are given by,

$$p_i(x) = -j\omega\rho\ u(x) = d_1[\ C_1\ h_1(a\ z) + C_2\ h_2(a\ z)], \quad (7)$$

$$v_i\ (x) = {}^{du(x)}/_{dx} = d_2[\ C_1\ h_1'(a\ z) + C_2\ h_2'(a\ z)] \quad (8)$$

where, $h_1'$and h_2' are the derivatives of the functions *h*1 and *h*2, respectively, and

$$a = \sqrt[3]{\frac{k_o}{A_c}},$$

$$d_1 = -j\ \omega\rho\ (\tfrac{9\ A_c}{4\ k_o})^{1/6} = -j\ k_o\ \rho c\ (\tfrac{9\ A_c}{4\ k_o})^{1/6},$$

and

$$d_2 = j\ (\frac{9\ k_o}{4\ A_c})^{1/6}$$

Such a treated duct, when it is applied, is usually inserted between two rigid ducts of equal cross-sections, Fig. 1. Considering this configuration, one can use the boundary conditions at the input of the treated duct, (*x*=0), namely the necessity of equal sound pressure and the continuity of sound flux, to determine the constants C1 and C2 of equations (7) and (8). On the other hand, the boundary conditions at the output of the treated duct (*x*=*l*), deliver the expression for the reflection coefficient *ri* and the normalized wave impedance (*Zo*/*ρc*) at the input of the duct. They are represented as:

$$|\ r_i\ | = -\left|\frac{N8+N10(1-N4)}{N10}\right|, \text{ and} \quad (9)$$

$$\left.\frac{Z_o}{\rho c}\right|_{x=0} = \mathcal{R}_o + j\ \chi_o = \frac{1+r_i}{1-r_i} \quad (10)$$

where;

$N_1 = d_1\ h_1\ (a.z_o) + \rho c\ d_2\ h_1'\ (a.z_o)$,
$N_2 = d_1\ h_2\ (a.z_o) + \rho c\ d_2\ h_2'\ (a.z_o)$,
$N_3 = h_1\ (a.z_o) - \frac{N1}{N2}\ h_2\ (a.z_o)$,
$N_4 = \frac{2d1}{N2}\ h_2\ (a.z_o)$,
$N_5 = \frac{N1}{2d1N3}$,
$N_6 = d_1\ h_1\ (a.z_l) - \rho c\ d_2\ h_1'\ (a.z_l)$,
$N_7 = d_1\ h_2\ (a.z_l) - \rho c\ d_2\ h_2'\ (a.z_l)$,
$N_8 = \frac{2N7}{N2}$, $N_9 = \frac{N6}{d1N3}$, and $N_{10} = N_9 - N_5.N_8$,

where, *zo* = - *ko.Ac*, and *zl* = *zo* + *j.l*

In a normal application, the MPP absorber is formed by placing the *MPP* in front of a rigid surface and with an air cavity of depth *D* in between. Therefore, the effect of an outside cavity chamber surrounding the parabolic increasing microperforated area was studied and computed. A locally reacting lining is characterized by the fact that there is no axial sound propagation within the lining. Accordingly, it is consumed theoretically and realized experimentally that the outside chamber is divided from the inside into many small chambers with rigid partitions at a small spacing between them, which is smaller than $\lambda/2$ of the highest frequency limit. The normalized acoustic impedance of the air cavity *Zc* behind the parabolic increasing microperforated area is defined as,

$$Z_c = -j\ \cot(\tfrac{\omega D}{c}), \quad (11)$$

Accordingly, the specific normalized impedance of the parabolic increasing microperforated area surrounded with an outside chamber of depth *D* is expressed as;

$$Z = Z_{MPP} - j\ \cot\left(\frac{\omega D}{c}\right) = R_m + j\ X_{mD}, \quad (12)$$

where

$$X_{mD} = X_m - \cot\left(\frac{\omega D}{C}\right)$$

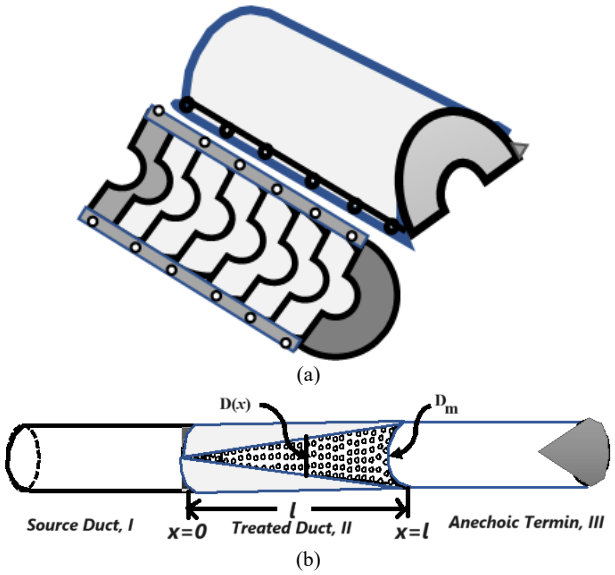

Fig. 1. Schematic diagram of the proposed duct system (a) Partitional outside cavity chamber and (b) Duct pipe system

3. Computed results

To study the matching performance of the treated duct to plane sound waves, the normalized wave resistance, *Ro*, the normalized wave reactance *Xo* of the normalized wave impedance and the sound reflection coefficient $|\boldsymbol{r_i}|$ at the inlet of the treated duct were computed. For these purposes a computer program in FORTRAN was prepared for estimating both sound reflection coefficient and sound wave impedance ($\mathcal{R}_o$ and χ_o) by estimating the values of *h*-functions and their derivatives *h`* by the substitution in equations, (9) and (10). In both cases, with and without the outside chamber, the effect of the following parameters and treatments on *Ro*, *Xo* and | *ri* | were computed;

- Effect of geometric parameters of the treated duct, namely; duct length, *l* and its cross-section, *S* (i.e. duct diameter, *Dp*)
- Effect of physical parameters of the *MPP*, from which the parabolic increasing area is produced, namely; thickness, *t*, hole diameter of perforation, *d* and perforation ratio (porosity), σ.
- Effect of *Rm* the normalized resistance and *Xm* (at 2000Hz as a guide) the normalized reactance of the normalized impedance *ZMPP* of the *MPP* with respect to their effect on each other.
- Effect of graduality, with which the parabolic increasing microperforated area is changed to produce *Dm* at the end of the treated duct.
- Effect of equal and similar multiple treatments that are distributed over the periphery of the treated duct side wall and are produced from the same *MPP* at constant total perforated area (sum of treated multiple areas).

For these purposes, different ducts of different *l* and *S,* that are treated with *MPP* of different physical parameters of *t*, *d* and σ were considered and computed for cases with and without outside chambers. Figs. 2(a) to (c), represent the computed *Ro*, *Xo* and | *ri* | as a function of frequency, *f*, for ducts of *l*= 50, 75 and 100 cm of the same diameter *Dp*= 5 cm when they were treated with a parabolic increasing microperforated area of maximum width *Dm*= 6.0 cm at the end of treated duct and which is produced from MPP of *t*= 1.0 mm, *d*= 0.3 mm and σ=2.0%. The figures show that:

- In general, at low frequency, both *Ro* and *Xo* increase with increasing *f* till they reach a maximum, then as *f* increases, *Ro* is reduced towards unity (i.e., *Ro*=ρc, is the air characteristic impedance) while *Xo* is reduced towards zero, in both cases with and without chamber, Figs. 2(a) and (b).
- It is also noticed that *Ro* reaches unity and *Xo* reaches zero at lower frequency *f* and still at these values as *l* increases. The figure shows also that | *ri* | decreases as *l* increases and reaches a reflection-free condition (i.e., | *ri* | ≤ 0.1) at a lower frequency as *l* increases, Fig. 2(c).

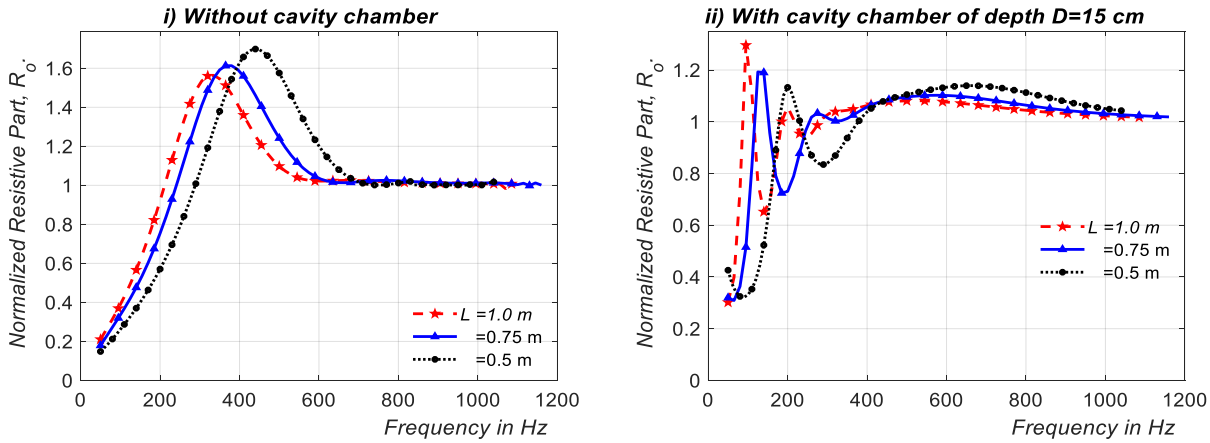

(a) Normalized wave resistive part of impedance at the inlet of the duct; (i) without chamber and (ii) with chamber

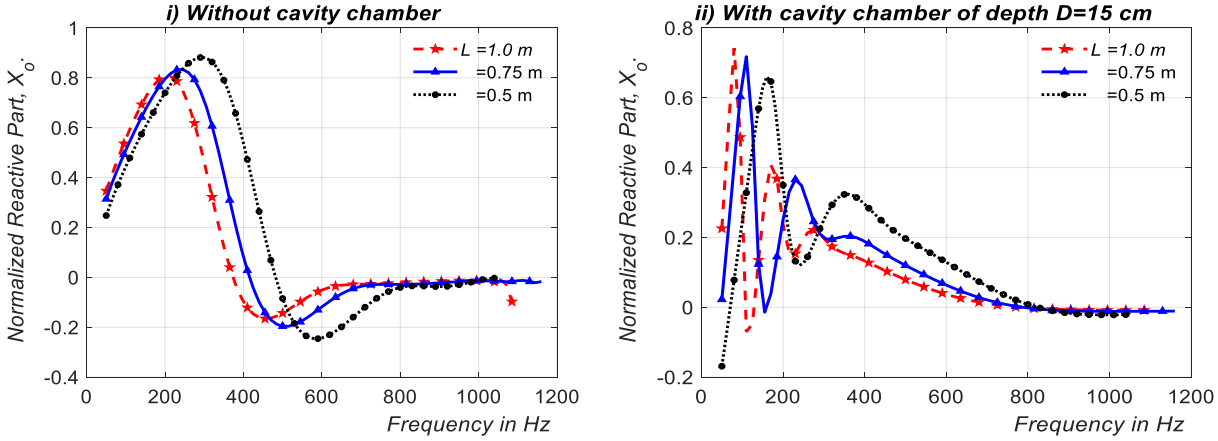

(b) Normalized wave reactive part of impedance at the inlet of the duct; (i) without the chamber, and (ii) with chamber

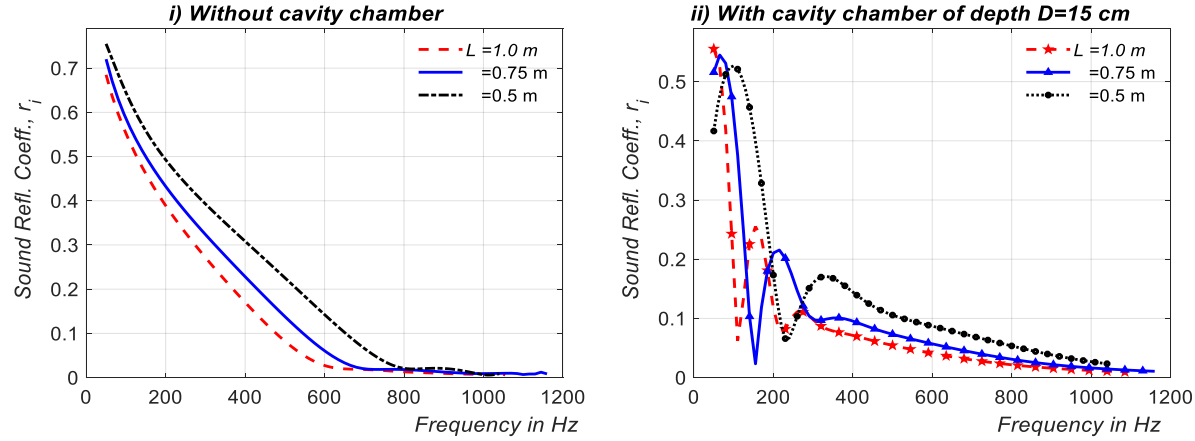

(c) Reflection coefficient of sound plane wave at the inlet of the duct; (i) without chamber and (ii) with chamber

Fig. 2. Effect of duct length, *l*=50, 75, and 100 cm; at *Dp*=5.0 cm, *Dm*=6.0 cm, *t*=1.0 mm, *d*= 0.3 mm and σ= 2%.

The graduality of wall conductance, which is defined as, the ratio between the maximum width of lining at the end of the treated part of the duct, *Dm* to the length of the treated part of the duct, *l* (i.e., Dm/*l*). Fig 2 shows that; | *ri* | reaches reflection-free condition at a lower frequency as the value, *Dm*/*l* decreases, which means that less change takes place in duct wall conductance of the treated duct at its inlet concerning the wall impedance of the rigid source duct. Also, the real part of impedance reaches unity while the imaginary part of impedance at the duct inlet reaches zero at a lower frequency, Figs. 2(a) and 2(b), respectively.

Fig. 3 represents the computed sound reflection coefficient in both cases without and with an outside chamber at the input of ducts of the same length *l*= 50 cm, but they have different cross-diameter *Dp*= 5.0, 7.5 and 10.0 cm. The ducts were treated with a parabolic increasing microperforated area of maximum width, *Dm*=6.0 cm, which are produced from MPP of *d*= 0.3 mm, *t*=1.0 mm and σ=2.0%. The figures show that | ***ri*** | reaches the reflection-free condition at a lower frequency as *Dp* increases.

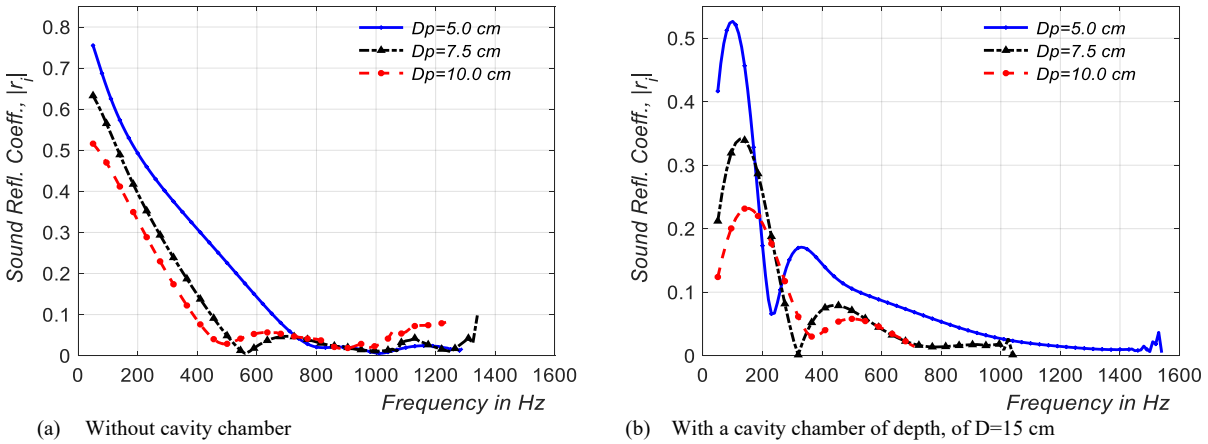

(a) Without cavity chamber (b) With a cavity chamber of depth, of D=15 cm

Fig. 3. Effect of cross-diameter, *Dp*=5, 7.5, 10cm; at *Dm* =6cm, ***t***=1mm, ***d***= 0.3mm and $\boldsymbol{\sigma}$= 2%.

Fig. 4 represents the computed | *ri* | as a function of frequency, *f*, for ducts of the same length *l*= 50 cm, and cross-section diameter *Dp*= 5.0 cm. The ducts were treated with a parabolic increasing microperforated area of maximum

width, *Dm*= 6.0 cm, which are produced from MPPs of *d*= 0.3 mm and σ=2.0%, but they have different *t*= 0.5, 0.75, 1.0 and 1.25 mm. The figures show that: | *ri* | reaches a reflection-free condition at a lower frequency as *t* increases for both cases with and without an outside chamber.

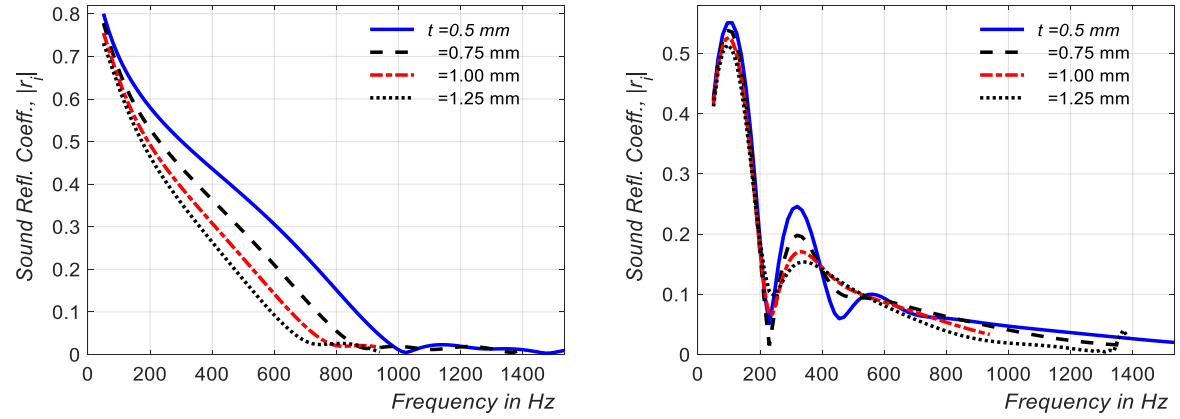

(a) Without cavity chamber (b) With a cavity chamber of depth, of D=15 cm

Fig. 4. Effect of *MPP* thickness, at *l*=0.5 m, *Dp*=5.0 cm, *Dm*=6.0 cm, ***d***= 0.3mm and $\boldsymbol{\sigma}$= 2%.

Fig. 5, represents the computed | *ri* | as a function of frequency, *f*, for ducts of the same length *l*= 50 cm, and cross-section diameter, *Dp*= 5.0cm. The ducts were treated with a parabolic increasing microperforated area of maximum width, *Dm*= 6.0 cm, which are produced from *MPPs* of the same *t*= 1.0 mm, and σ= 2.0%, but they have different, *d*=0.2, 0.3, 0.4 and 0.5mm. The figures show that; | *ri* | decreases by decreasing *d*, and reaches the reflection-free condition at a lower frequency as *d* decreases, for both cases with and without an outside chamber.

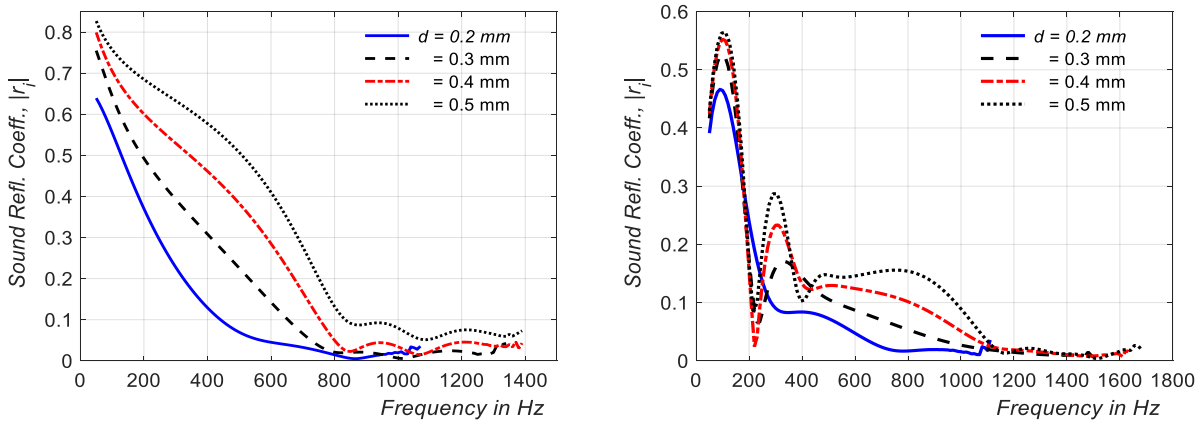

(a) Without cavity chamber (b) With a cavity chamber of depth, of D=15 cm

Fig. 5. Effect of MPP hole diameter, ***d***: at ***l***=0.5 m, *Dp*=5 cm, *Dm*=6 cm, ***t***= 1.0 mm and $\boldsymbol{\sigma}$= 2 %.

Fig. 6, represents the computed | *ri* | as a function of frequency *f*, for ducts of the same length *l* = 0.5 m, and cross-section diameter, *Dp*= 5.0 cm. The ducts were treated with a parabolic increasing microperforated area of maximum width, *Dm*= 6.0 cm, which are produced from *MPPs* of the same, *t*= 1.0 mm, *d*= 0.3 mm, but they have different, σ=1.0, 2.0, 3.0 and 5.0%. The figures show that; |*ri*| decreases by decreasing σ, and reaches a reflection-free condition at a lower frequency as σ decreases, for both cases with and without an outside chamber. The above-computed results indicate that the best matching performance to plane sound waves, namely, *Ro* =1, *Xo* =0 and | *ri* | ≤ 0.1 can be realized at lower frequencies by increasing *l*, *Dp*, *t* and also, by decreasing *d* and σ.

To study the effect of the normalized resistive part *Rm* and the normalized reactive part *Xm* of the *MPP* normalized impedance, *ZMPP*. with respect to each other on the matching performance to plane sound waves, different ducts with different treatments were considered and computed. The ducts have the same lengths, *l*=0.5 m and the same cross-diameter *Dp*=5.0 cm and they are treated on their side walls with parabolic increasing microperforated areas with graduality that realize the same *Dm*= 6.0 cm. These areas are produced from different *MPP*s that realize; *Xm* < *Rm*; *Xm* = *Rm*; and *Xm*> *Rm*, (at 2000 Hz as a guide). The computed results are represented in Fig. 7, we can conclude that the best matching performance at *Xm* ≤ *Rm*.. The values of *t*, *d* and σ that can be realized in these conditions as examples as follow;

- *Xm* < *Rm* represent by MPP-I, which produced from MPP of *t*= 1 mm, *d*= 0.16 mm and σ = 6 %, which realize *Rm*=1.0 and *Xm* = 0.5 (at *f*=2000 Hz as guide)
- *Xm*= *Rm* represented by MPP-II, which is produced from MPP of *t*=0.75, *d*= 0.175 mm and σ =4.0%, which realizes *Rm*=1.0 and *Xm*= 0.981.
- *Xm* > *Rm* is represented by MPP-III, which is produced from MPP of *t*= 1.0 mm, *d*= 0.27 mm and σ =2.5 %, which realize*s* *Rm*=1.0 and *Xm* =2.05.

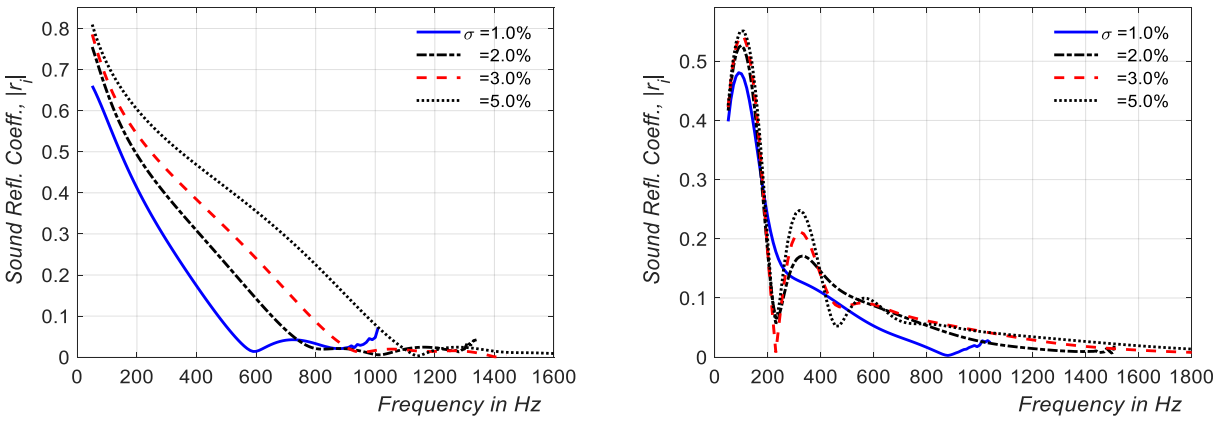

(a) Without cavity chamber (b) With a cavity chamber of depth, of D=15 cm

Fig. 6. Effect of MPP perforation ratio, σ, l=0.5m, Dp=5cm, Dm=6cm, t=1.0mm and d=0.3mm.

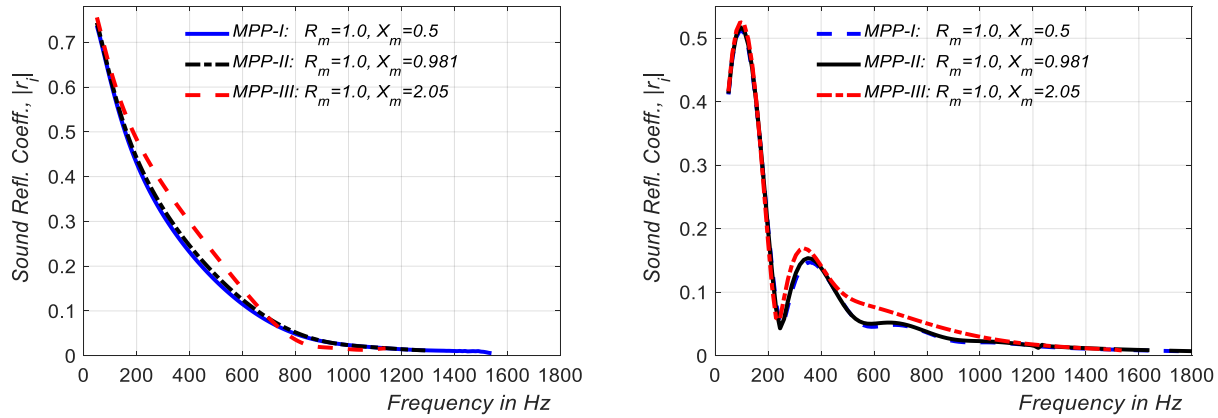

(a) Without cavity chamber (b) With a cavity chamber of depth, of D=15 cm

Fig. 7. Effect of *Rm* and *Xm* relative to each other on sound reflection of ducts have, l = 0.5 m, at Dp=5.0 cm, Dm= 6.0 cm, and have different t's, d's and σ's

4. Multiple Treatment

To study the effect of multiple treatments on the matching performance of the proposed duct to a plane sound wave, the acoustic image principle is applied. This can be achieved by treating the duct at its side wall and along its whole length with multiple equal and similar side parabolic increasing microperforated areas (i.e., n times treatments), which are distributed over the periphery of the treated duct. In this case, the cross-section area, S of the treated duct is considered as S/n, for each treatment. Accordingly, the characteristic area of the treated duct becomes, $A_C = \frac{S\,.l.Z_{MPP}}{n\,D_{mn}}$, where: n is the number of similar treatments, and *Dmn* is the maximum width of the parabolic increasing microperforated area at the end of the treated duct for each treatment.

For this purpose, ducts of length l = 0.5 m. of cross-diameter Dp= 5.0 and 1.0 cm were treated and computed. These ducts are treated with parabolic increasing microperforated area with graduality that produces different *Dm* -values. These areas are produced from the same *MPP* of t = 1.0 mm, d= 0.3 mm and σ =2.0 %. The number of treatments n and the graduality, which is applied to produce different *Dm*-values for different *Dp* are:

- For Dp= 5.0 cm: Dm=6.0 cm for n=1; Dmn=3.0 cm for n=2; and Dmn=2.0 cm for n=3.
- For Dp= 10 cm: Dm=12 cm for n=1, Dmn=6cm for n=2, Dmn=4 cm for n=3 and Dmn=3 cm for n=4.

The computed results are represented in Fig. 8(a), for Dp= 5.0 cm and Fig. 8(b) for Dp=10 cm. The figures show that; The best matching performance that $|ri| \leq 0.1$ realizes at a lower frequency for a single treatment, while it is shifted a little to high frequency as the number of treatments n increases, since the effective cross-section area S/n. Accordingly, the cross-diameter of the treated duct becomes narrower and the reflection coefficient increases. Comparing the cases for n=1, in Fig. 8(a) with n= 2, in Fig. 8(b) and also, comparing cases for n=2 in Fig 8(a), with n = 4, in Fig 8(b), it can be noticed that they are identical in accordance to the sound image principle. This is due to the effective cross-section area S/n of the different treatments.

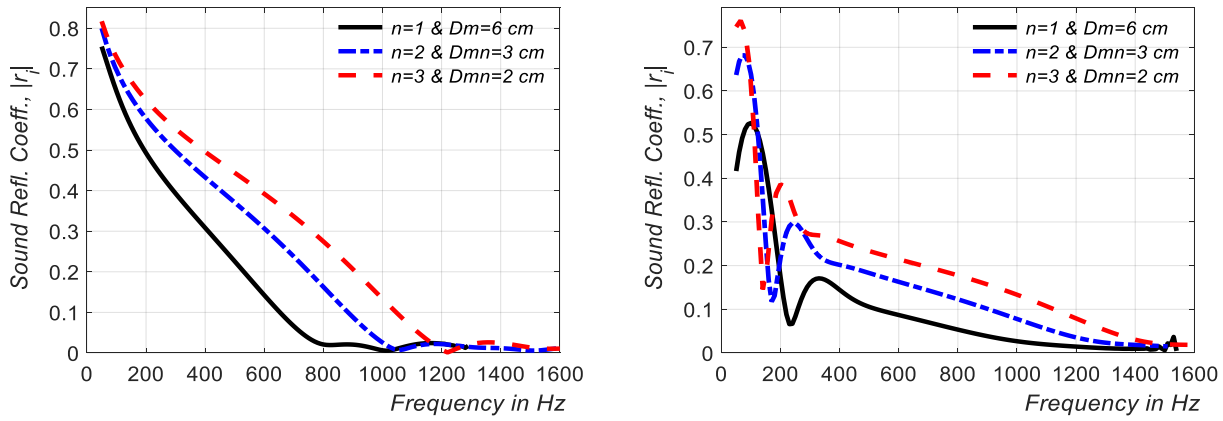

(a) Reflection coefficient of plane waves, at duct inlet for ***Dp***= 5 cm; (i) without chamber and (ii) with cavity chamber.

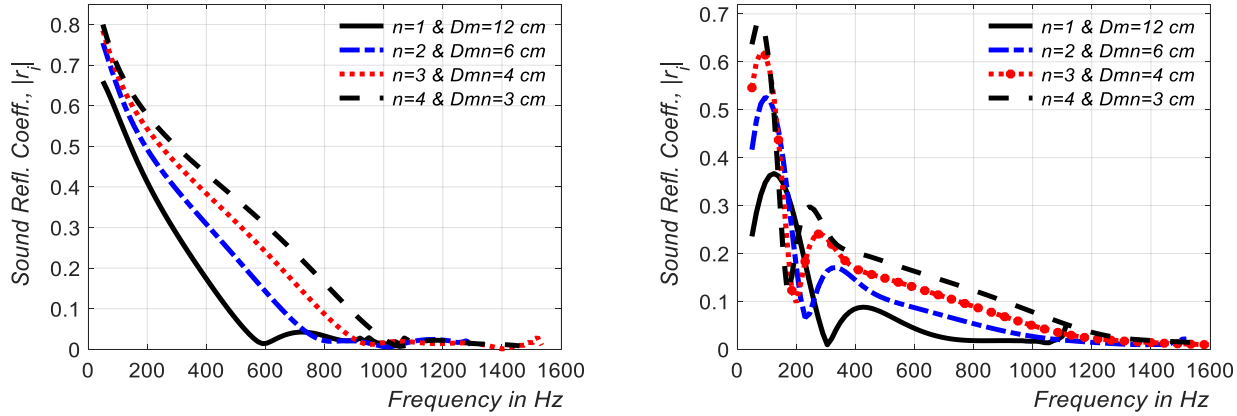

(b) Reflection coefficient of plane waves, at duct inlet for *Dp*=10 cm; (i) without chamber and (ii) with cavity chamber.

Fig. 8. Effect of multiple treatments using *MPP*, for ducts have ***l***=0.5m, ***t***=1.0 and *d*=0.3mm and σ=2.0%.

5. Experimental Verifications

5.1. Measuring Arrangement

Experimental studies are carried out to validate the theoretical model. The examined duct consists of a free path rectangular duct with an inside dimensional 10.0 cm (duct height) by 7.0 cm (duct width) that gives cross-section, *S rectangular* =70 cm2 and different duct lengths, ***l***= 0.5 and 1.0 m. The parabolic increasing microperforated area of *Dm*= 6.0 cm is made on the small side width, 7.0 cm. This area is produced from an MPP which is made of stainless steel of geometrical parameters; ***t*** = 0.65 mm, ***d***= 0.45 mm and $\boldsymbol{\sigma}$ =2.0 %. The treated duct side with the parabolic increasing microperforated area is covered with a partitioned air cavity chamber of depth 15.0 cm and width 7.0 cm. The chamber is divided from the inside with rigid partitions in spacing 7.0 cm to satisfy the local reacting lining in the measuring frequency range. The duct walls and the outside cavity chamber are made from wood of thickness 2.0 cm. The largest cross-dimension, 10 cm allows plan sound waves with frequency up to 1700 Hz to propagate in the test duct. Fig. 9 shows the experimental measuring arrangement. The experimental designed rig is based on the two-microphone method, according to ISO-10534-2 [32] and ASTM E1050-12 [33].

A Bruel & Kjaer Type 4206 is used in the measurements. A loudspeaker is mounted at one side of the source duct while the other side of the source duct is attached to the inlet of the treated duct, Fig. 9. Random noise signal covers the interested frequency range produced from the analyzer generator type 2035, is fitted to the loudspeaker through B&K power amplifier type 2706. Measurements are made with two 1/4″ condenser microphones B&K 4187 with preamplifier type 2670, and application software BZ5050 which allows control measurement through the IBM PC using B&K Type 2035.

5.2. Realization of parabolic increasing microperforated area

The parabolic increasing microperforated area can be realized using a slit, which changes parabolically along the length of the treated duct. This slit reaches a maximum width *Dm* at the end of the treated duct (duct outlet, ***x=l***). From the acoustical point of view, this slit can be replaced by a microperforated area, which is produced from MPP within the slit boundaries. In applications, when sound radiation is not allowed, as in exhaust silencers, and also to prevent the flow of gases travelling in the duct to the surroundings, for example in air conditioning ducts, an outside chamber of suitable depth can be used.

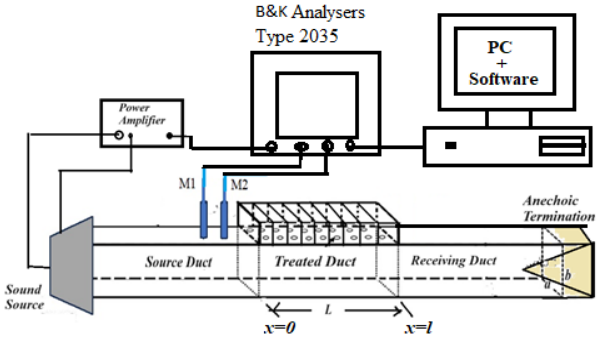

Fig. 9. Schematic diagram of the sound measurement rig.

5.3. Experimental results

Figs. 10(a) and (b) show a comparison between the measured and computed sound reflection coefficient for rectangular ducts of cross-section area 70 cm2 (width=7 cm and height=10 cm) and lengths 0.5 m and 1.0 m. These ducts are lined with parabolic increasing microperforated areas of maximum width, *Dm*= 6.0 cm, which are produced from MPP of ***t*** = 0.65 mm, ***d*** = 0.45 mm and σ=2.0 %. Figures show that the computed and the measured sound reflection coefficients for the two computed lengths (*l*= 0.5 m and *l*= 1.0 m) are in agreement. The difference in sound reflection coefficient is about 0.05, in the presence of the outside air cavity chamber, while in the case of the absence of the outside air cavity chamber, the difference is slightly high and reached 0.1, especially at very low frequencies (*f*<100Hz).

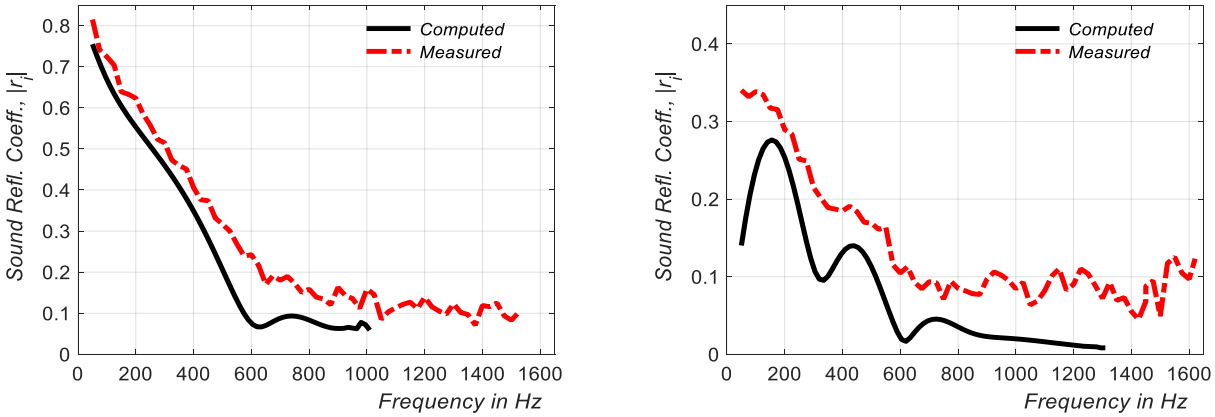

(a) Duct length, ***l***= 0.5 m; i) without chamber and ii) with outside cavity chamber

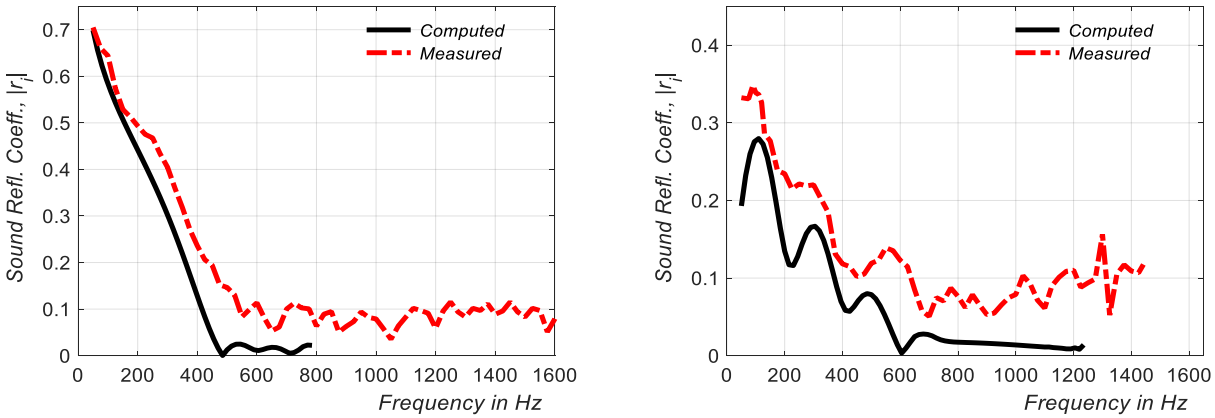

(b) Duct length, ***l*** = 1.0 m; i) without chamber and ii) with outside cavity chamber

Fig.10. Comparison between computed and measured sound reflection for ducts lined with MPP of *t* = 0.65 mm, *d* = 0.45 mm and *d* = 2.0 %

6. Critical analysis of the proposed duct design

The proposed duct design provides the solution for the two main factors that are responsible for the mismatching through the duct namely; the duct cross-section discontinuity and the abrupt change in wall conductance of the treatment ducts.

In comparison between constant treatments that have parabolic increasing lining along the duct, two ducts have the same length of 0.5m and the same MP liner areas are used, one of constant slit of 3.5cm width, and the other with parabolic increasing of maximum width 5.25cm (The area of a parabola is equal 4/3 times the area of the triangle having as vertices the two intersecting points). The two ducts are tested experimentally and the measured data are represented in Fig. 13. The comparative results show that the reflection coefficient of the constant slit lining is much higher than that of the same liner area of the parabolic lining duct, with about an average 0.1 over the range frequency from 50 Hz to 850 Hz (i.e. more than 5 Octave that covers very low- and mid-frequency range). The higher sound reflection for the constant slit lining is due to the abrupt change in the duct wall conductance and consequently, causes an abrupt change in the duct lining acoustic impedance.

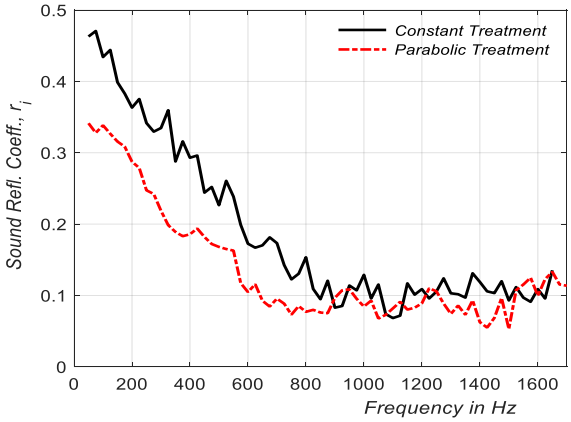

Fig. 11. Experimental comparison of sound reflection between constant lining duct and parabolic increasing lining one having the same length and the same perforation areas.

Additionally, a comparison between traditional perforation and micro-perforation MP lining treatments is studied. Three ducts have the same graduality and the same length, but they have different orifices diameters (***d***1=0.3mm, ***d***2=0.5mm and ***d***3=1.2mm) are considered, and the obtained results are represented in Fig. 12. The computed results show that the

matching performance for micro-perforation lining treatment is better than that for the normal perforation (orifices diameter is greater than or equal 1.0mm) lining treatment. It was found that the reflection coefficient for micro-perforation lining is smaller by about 0.2 in the frequency range from 50 Hz to 1.0 kHz (about 6 Octave bands). This is due to that the MPP liner is highly resistive and consequently, it highly absorbs sound energy and low reflected sound energy.

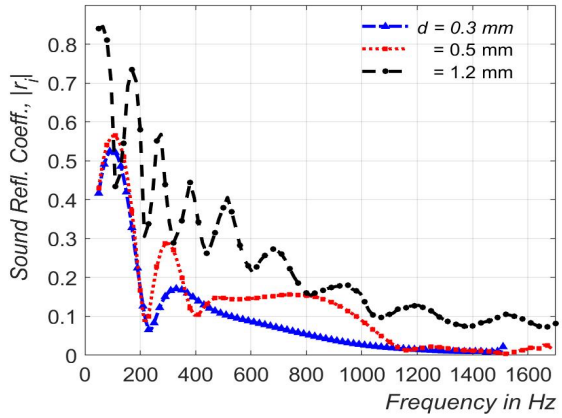

Fig. 12. Sound reflection comparison between MPP and normal perforation lining

7. Suggested application model for exhaust silencer

The treated duct in the present work was previously studied as a sound attenuator by the authors (Shenoda and Elaidy, 2023). It was found that it provides high sound transmission loss in a wide frequency band (about 3.5 octaves). The previous study showed that it can be designed to be effective in the low frequency- band or the mid-and high-frequency band by proper selection of the MPP. Since the present study showed also that this type possesses a small reflection coefficient at its inlet if it is inserted between two similar hard ducts, it can be applied as an exhaust silencer for the following reasons:

- It has a free path constant cross-sectional area without any discontinuities
- It can be designed from metal sheets without using any fibrous materials which means that it is clean, non-combustible, recyclable and suitable for applications in a high-temperature environment. In addition, it has a low volume and long lifetime.
- It can be designed with a cross-section area similar to that of the exhaust pipe and accordingly, a very small sound reflection takes place at its inlet, which means minimum back pressure and accordingly, minimum power loss which leads in turn to minimum fuel consumption.

Two models are suggested, namely; Silencer model S-I, which is designed with a single treatment and model, S-II, which is designed with double treatments. Fig. 13a shows the schematic diagram of a single treatment and Fig. 13b, shows the computed sound reflection coefficient and the computed sound transmission loss [10]. The schematic diagram of the double treatments silencer model, S-II is represented in Fig. 14a, and the computed results are shown in Fig.14b.

It is noticed that the single treatment model S-I, gives lower sound reflection over a wide frequency range with acceptable sound transmission loss. In contrary the double treatments silencer model S-II gives higher sound transmission loss and acceptable sound reflection.

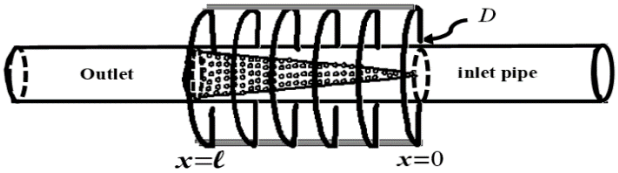

(a) Schematic Diagram of the single treatment model, S-I

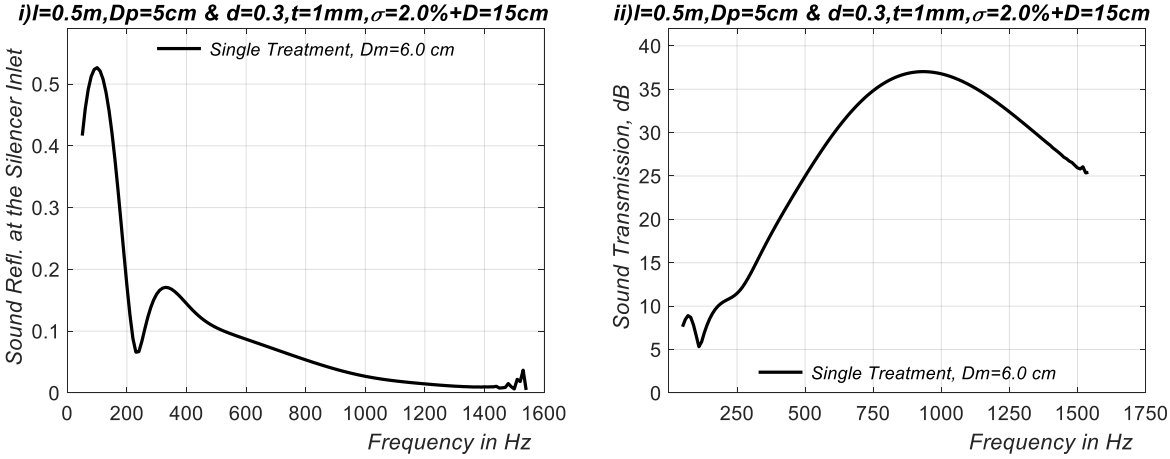

(b) Computed results: i) Sound reflection and ii) Sound transmission loss due to silencer

Fig.13. Single treatment silencer model, S-I.

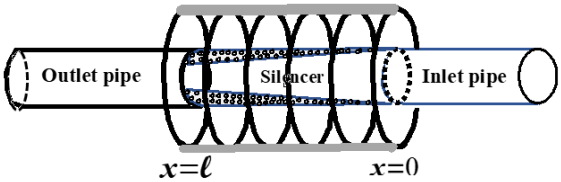

(a) Schematic Diagram of a double treatments silencer model, S-II.

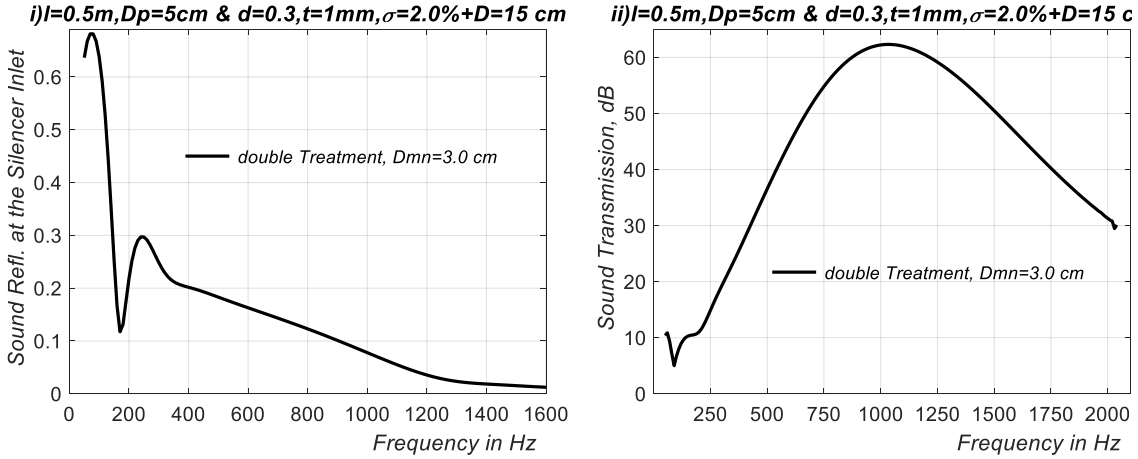

(b) Computed results: i) Sound reflection and ii) Sound transmission loss due to silencer.

Fig. 14. Double treatments silencer model, S-II.

8. Conclusion

In this study, a kind of liner material, MPP has been used in the lining of the duct that is treated with variable wall conductance along the duct length which was suggested by Shenoda [17], with emphasis on its various applications. It was found that the MPP liner has certain advantages over the duct treated and lined with the normal perforations, especially, the associated improvements for the matching performance in the case of ducts lined with the MPP liner of variable wall conductance treatment. The effects of the duct parameters, as well as, the physical parameter of the lining MPP effects on the sound reflection and impedance matching were analyzed and discussed. The study came up with the following conclusions:

1) The sound reflection coefficient produced at the inlet of a duct lined with MPP liner is less by about 0.2 than that is produced by a normal perforation liner at low- and mid-frequency ranges (from 50 Hz to 1.0kHz).
2) The sound reflection coefficient produced at the inlet of a duct lined with a parabolic increasing MPP area along the duct is lower by about 0.1 than that is produced by a constant slit treatment along a duct with MPP liner at low- and mid-frequency ranges (from 50 Hz to 850Hz).
3) The sound reflection coefficient at the inlet of the treated duct decreases with increasing the duct length, *l*, duct cross-section *Dp*, the MPP thickness, *t* and by decreasing the hole perforation diameter *d* and perforation ratio σ of the MPP.
4) It was found also, that good matching performance to plane sound waves incident at its input can be realized by decreasing the graduality with which the microperforated area changes to realize *Dm* for a single treatment and when the reactive part of the MPP-impedance *Xm* is less or equal to its resistive part *Rm* ($Xm \leq Rm$).
5) Having a free path and a constant cross-sectional area, this duct can be applied:
   a. As anechoic termination for machine testing in duct method or as an attenuator of air conditioning ducts.
   b. This type of treated duct
      i. It provides a high level of sound attenuation over a wide frequency range with significant low-frequency attenuation within a small volume [25].
      ii. Its noise control depends principally on geometrical considerations is independent of the kind and performance of the noise source and has no influence on its performance.
      iii. It is made of metal sheet and accordingly, it is non-combustible, recyclable, suitable for application in high-temperature environments and has a long lifetime

   Therefore, it can be applied as an exhaust silencer, which realizes low back pressure and low power loss to continuous or pulsating gas flow, which leads in turn to lower fuel consumption.
6) The experimental results successfully verified the validity of the theoretical model.
7) To realize a high attenuation over a wide frequency range with acceptable matching performance multiple-treatment can be applied.

References

[1] R. Ballesteros-Tajadura, R. S. Velarde-Suarez, and J. P. Hurtado-Cruz, "Noise prediction of a centrifugal fan: numerical results and experimental validation," *J. Fluids Eng.*, vol. 130, no. 9, pp. 1-12, Sep. 2008.

[2] L. L. Beranek, Ed., *Noise and vibration control*, Rev. ed. Washington, DC: Inst. of Noise Control Engineering, 1988.

[3] U. Kurze, "Schallabsorbierender Kanal," Diplomarbeit, Institute fuer Techn. Akustik, TU Berlin, 1962.

[4] J. W. Sullivan, and M. J. Croker, "Acoustic analysis of dissipitive silencers using numerical models obtained by the technique of Transfer Matrix and the Finite Element Method," *J. Acoust. Soc. Am.*, vol. 64, no. 1, p 207-217, Jan. 1978.

[5] F. Rafique, J. H. Wu, C.R. Liu, and F. Ma, "Transmission Loss analysis of a simple expansion chamber muffler with extended inlet and outlet combined with inhomogeneous micro-perforated panel (iMPP)," *Appl. Acoust.*, vol., 194, Art. no. 108808, Jun. 2022.

[6] E. Zhuravlev, D. Chugunkov, and G. Seyfelmlyukova, "Improving the acoustic efficiency of laminated dissipative noise silencers for boiler gas-air paths," *E3S Web Conf.*, vol. 140, Art. no, 02005, 2019, doi: 10.1051/e3sconf/201914002005.

[7] V. Pagneux, N. Amir, and J. Kergomard, "A study of wave propagation in varying cross-section waveguides by modal decomposition," Part I. Theory and validation," *J. Acoust. Soc. Am.*, vol. 100, no. 4, pp. 2034–2048, Oct. 1996.

[8] A. H. Nayfeh, J. E. Kaiser, R. L. Marshall, and C. J. Hurst, "A Comparison of experiment and theory for sound propagation in variable area ducts," *J. Sound and Vib.*, vol. 71, no. 2, pp. 241-259, Jul. 1980.

[9] E. Bängtsson, D. Noreland, and M. Berggren, "Shape optimization of an acoustic horn comparison methods," *Appl. Mech. Eng.*, vol.192, no. 11, pp. 1533–1571, Mar. 2003.

[10] H. Dong, Y. Shen, and H. Gao, "Shape optimization of acoustic horns using the multimodal method," *J. Acoust. Soc. Am.*, vol.147, no. 4, pp. 326 – 332, Apr. 2020.

[11] W. E. Zorumski, "Generalized radiation impedances and reflection coefficients of circular and annular ducts," *J. Acoust. Soc. Am*, vol 54, no. 6, pp. 1667–1673, Dec 1973.

[12] J.-P, Dalmont, and E. Portier, "Optimisation of anechoic duct termination using line theory," *Appl. Acoust.*, vol. 117, part A, pp. 141-144, Feb. 2017.

[13] P. Dickens, J. R. Smith, and J. Wolfe, "Improved precision in measurements of acoustic impedance spectra using resonance-free calibration loads and controlled error distribution," *J. Acoust. Soc. Am.*, vol. 121, no. 3, pp.1471-81, Apr. 2007.

[14] F. B. Shenoda, "Anechoic termination for air ducts," VDI-*Gemeinschaftstagung Akustik und Schwingungs-Technik*, *DAGA Stuttgart*, pp. 269-272, 1972.

[15] F. B.Shenoda, and H. Ising, "A power increasing exhaust silencer for racing cars," *Kampf den Laerm*, vol. 25, pp. 123-126, Sep. 1978.

[16] F. B.Shenoda, H. Wal, and A. Meier. "Dissipative silencers with minimized back pressure," *INTER-NOISE and NOISE-CON Congr. Conf. Proceed., Inst. Nois. Cont. Engin.*, pp. 297-302, Aug. 1981.

[17] F. B. Shenoda, "A new silencer with good matching performance for air ducts and exhaust systems," *Acta Acust. unit. Acust.*, vol. 50, no. 5, pp. 338-341, May 1982.

[18] F. B. Shenoda, "Exhaust silencers with minimum power loss," *Arch. Acoust.*, vol. 11, no. 2, pp. 137-150, Feb. 1986.

[19] R.J. Astley and W. Eversman, "A Finite Element Method for transmission in non-uniform ducts without flow: Comparison with the method of weighted residuals," *J. Sound and Vib*., vol. 57, no.3, pp. 367-388, Apr. 1978.

[20] R.J. Astley, and A. Cummings, "A Finite Element Scheme for attenuation in ducts lined with porous material: Comparison with experiment," *J. Sound and Vib*., vol. 116, no. 2, pp. 239-263, Jul. 1987.

[21] Chaoxian Qi, Shubin Zeng, and Jiefu Chen, "Analysis of sound propagation across acoustic ducts with discontinuities using a high precision finite element method," *IEEE J. Multisc. Multiph. Computat. Techn.*, vol. 7, pp. 36 – 45, Feb. 2022.

[22] C. Y. R. Cheng, A. F. Seybert and T. W. Wu, "A Multi-domain Boundary Element solution for silencer and muffler performance prediction," *J. Sound Vib.*, vol.151, pp. 119–129, Nov. 1991.

[23] A. F. Seybert, R. A. Seman, and M. D. Lattuca, "Boundary Element Prediction of sound propagation in ducts containing bulk absorbing materials," *J. Vib. Acoust*., vol.120, no, 4, pp. 976-981, Oct. 1998.

[24] H. Utsuno, T. Tanaka, T. Fujikawa, and A.F. Soybert, "Transfer Function Method for measuring characteristic impedance and propagation constant of porous materials," *J. Acoust. Soc. Am.*, vol. 86, no. 2, pp. 637–643, Aug. 1989.

[25] W. Xiaoyu, and S. Xiaofeng, "Transfer Element Method with application to acoustic design of aeroengine nacelle," *Chin. J. Aeronautics*, vol, 28, no. 2, pp. 327–345, Apr. 2015.

[26] D. Herrin, J. Liu, and A. Seybert, "Properties and applications of microperforated panels," *Sound & Vib.*, vol. 45, no. 1, pp. 6-9, Jul. 2011.

[27] F. B. Shenoda, and M. El Aidy, "An effective broadband frequency sound attenuator duct lined with parabolic increasing microperforated area," (under publication)

[28] D. Y. Maa, "Theory and design of microperforated panel sound-absorbing constructions," *Scient. Sin.*, vol. 18, no. 1, pp. 38-50, Jan. 1975.

[29] D. Y. Maa, "Potential of microperforated panel absorber," *J. Acoust. Soc. Am.*, vol. 104, no. 5, pp. 2861-2866, Nov. 1998.

[30] G. N. Watson, *A Treatise on the Theory of Bessel Functions*. New York: MacMillan, 1944.

[31] The Staff of the Computation Laboratory, *Modified Hankel-Functions of order One-Third and their derivative*, Cambridge Mass. Harvard Uni. Press, vol. II, 1945.

[32] ISO 10534-2, *Determination of Sound Absorption Coefficient and Impedance in Impedance Tubes*, ISO 10534-2. 1998.

[33] *Standard Test Method for Measurement of Normal Incident Sound Transmission of Acoustical Materials Based on Transfer Matrix Method*. ASTM E2611-09, 2009.